# 3D Seismic Numerical Modeling of Infrastructure on Liquefiable Soils - Soil-Structure Interaction and Soil-Cement Grid Modeling

Viet (Victor) Tran, PhD, P.Eng., PMP
Principal Geotechnical Engineer, FECON Geotechnical Ltd., Port Coquitlam, BC
Email: victor@fecongeo.com

**ABSTRACT** 3D seismic numerical modeling using the FLAC3D program was carried out for three representative cases: 1) an embankment dam on a liquefiable layer, 2) a berth structure consisting of quay wall supported by anchor walls and tie-rods subject to soil liquefaction, and 3) a long pier consisting of vertical and battered steel pipe piles supporting deck structures. Soil-cement grids were considered in case 2 to mitigate liquefaction effects. The P2PSAND soil constitutive model, specifically designed for 3D modeling of liquefied soils, was employed to represent liquefiable soils. The P2PSAND model is based on the framework of the DM04 model and is a critical-state compatible and plasticity model utilizing bounding surface theory. The model can simulate non-linear response, liquefaction triggering and strength reduction of the soils during earthquake. Soil-cement grids of various sizes were modeled in 3D to evaluate the method's efficiency to reduce liquefaction and provide insight into the performance of the system. The structures were simulated with their 3D geometries to best evaluate the 3D soil and structure interaction. The effects of the earthquake direction, seismic wave propagation to surface, and sizes of soil-cement grids were also presented and discussed.

## Introduction

Embankments and marine structures are often located on steep river or marine slopes where subsurface soils can become liquefiable. These conditions frequently lead to significant deformations in both the soil and the structures. Typical design may involve 2D geotechnical seismic ground deformation analysis followed by seismic structural design. Post-seismic soil deformation along with p-y curves are often provided to the structural engineer to account for the kinematic effects. However, this structural assessment is often decoupled from the geotechnical analysis. While this process is straightforward, the ground deformation and the relatively simplistic p-y curves do not comprehensively capture the intricate soil-structure interaction during earthquakes. Moreover, 2D geotechnical modeling, although practical, often fails to adequately represent the three-dimensional (3D) characteristics of structures and ground reinforcement.

There are several soil constitutive models that have been widely used for soil liquefaction modeling. Nevertheless, most of these models are limited to two dimensions. Recent advancements have introduced new 3D soil models, such as P2PSand, which is available within the FLAC 3D program. This study aims to leverage the capabilities of this 3D soil model for simulating liquefaction. By utilizing the FLAC 3D program, this research will delve into the realm of 3D soil and structure interaction, shedding light on the seismic response of both soils and structures.

## Soil Constitutive Model

Multiple soil models have been developed to simulate the soil liquefaction of sand-like materials in geotechnical earthquake engineering. Among the prominent models are the PDMY model (Elgamal et al., 2003; Yang et al., 2003), DM04 model (Dafalias and Manzari, 2004), SANISand model series (Taiebat and Dafalias, 2008; Yang et al., 2022), NTUA sand model (Papadimitriou and Bouckovalas, 2002), UBCSand model (Beaty and Byrne, 2011), and PM4Sand model (Boulanger and Ziotopoulou, 2015).

In practical geotechnical earthquake modeling, two widely utilized 2D constitutive models are UBCSAND and PM4SAND. These models are available in several geotechnical software programs, although they are exclusively applicable to 2D plane strain conditions. More recently, to address the growing need for a 3D soil model capable of simulating soil behavior under seismic conditions, the P2PSAND model was introduced by Cheng and Detournay (2021).

The P2PSand model stands as a practical 3D two-surface plastic constitutive model founded on the DM04 model. This model encompasses both the theoretical robustness of the PM04 model and the pragmatic features of the UBCSand and PM4Sand models. Furthermore, the P2PSand model has been integrated into the commercially available geotechnical program FLAC3D. For further theoretical insights into the model, readers are directed to Cheng and Detournay (2021).

## P2PSand Model Calibration

The model has been numerically calibrated to the liquefaction triggering curve proposed by Idriss and Boulanger (2008) as shown in Figure 1a. The numerical calibration was based on element CDSS (cyclic direct simple shear) test simulation and the CSR (cyclic stress ratio) was calculated based on the shear stress required to reach liquefaction after 15 equivalent cycles. Liquefaction was defined as excess pore water pressure ratio reaching 98% or maximum shear strain reaching 3%. The profiles of CSR versus number of cycles to liquefaction (N) are presented in Figure 1b. Representative DSS stress-strain responses of the P2PSand model are shown in Figure 2. The results are from element CDSS tests under undrained stress-controlled loading conditions.

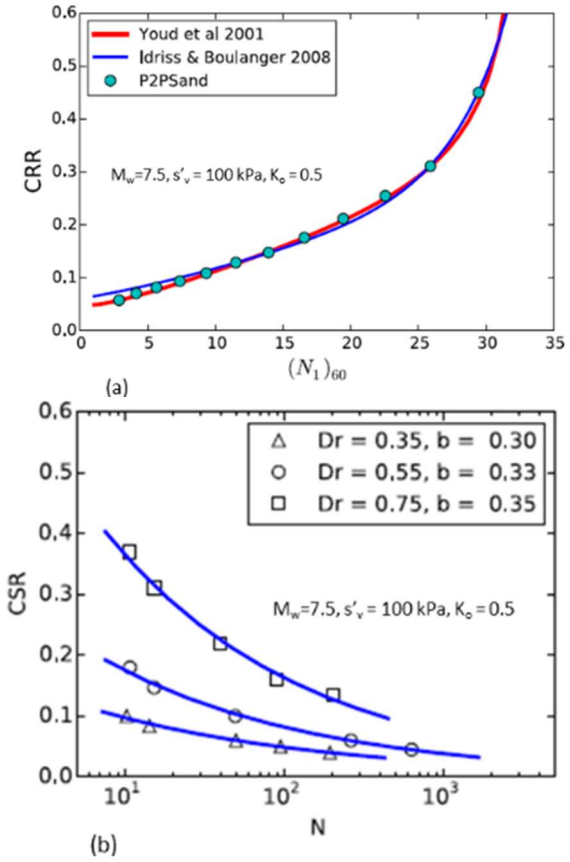


**Fig. 1**. P2PSand model numerical calibration: (a) Liquefaction triggering curve, (b) CSR – N relationship (adopted from Cheng and Detournay, 2021)

The primary input parameters of the P2PSand model are relative density (Dr) and soil densities. The small-strain shear modulus (G) is calculated using the following equation:

[1] $$G = f(D_r)P_a\left(\frac{p'_m}{P_a}\right)^2$$

where: $f(D_r)$=1.24e$^3$$(D_r + 0.01)$, $P_a$ is atmospheric pressure taken as 100 kPa, and $p'_m$ is the soil mean effective stress. The constant volume friction angle $\phi'_{cv}$ of 33 degrees and $K_o$ (the ratio of horizontal effective stress to vertical effective stress at the start of loading) of 0.5 were used. All other parameters are default or internally calibrated.

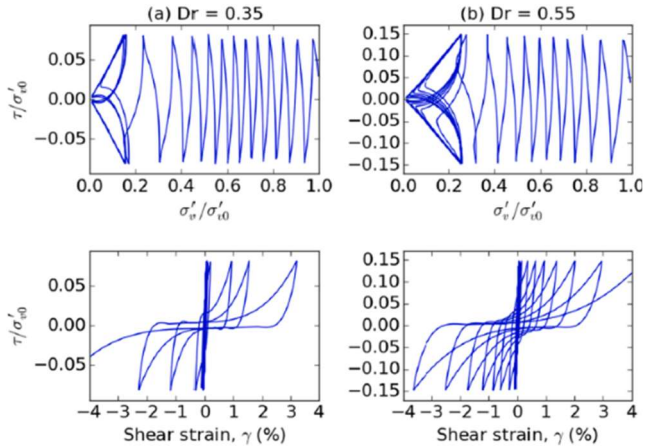


**Fig. 2**. Stress – strain relationship – P2PSand model CDSS testing (adopted from Cheng and Detournay, 2021)

# Case Study 1: Embankment Dam on Liquefiable Layer

## Embankment Model

In this case study, we employed the FLAC 3D program (v7, Itasca Consulting) to model a road embankment situated along a riverbank. The top of the embankment is at El. -15 m. A densified sand and gravel fill with a thickness of 3 m was placed beneath the embankment surface. Below the fill soils, a layer of dense sand extended to El. – 6 m was encountered, which is underlain by a loose sand layer. This loose sand layer has a thickness of 12 m and overlying a sand and gravel layer. Along the riverside, the embankment boasts a slope of 2H:1V, succeeded by a flat bench at an elevation of 0 m, spanning a width of 20 m. A 2H:1V river slope is then extended to reach the riverbed at an elevation of -6 m. A water level set at an elevation of 0 m was considered within the model. The geometrical configuration of the embankment is illustrated in Figure 3.

Particularly noteworthy is the susceptibility of the sand soils, especially the loose sand layer, to liquefaction during seismic events. To capture this behavior, the P2PSAND model was employed for modeling these soil strata. The pertinent soil parameters are detailed in Table 1.

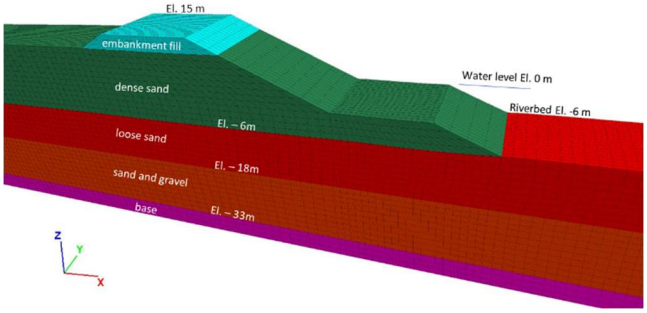


**Fig. 3.** Embankment geometry

**Table 1**. Soil parameters – case study 1

| Soil layer | Unit weight (kN/m$^3$) | Relative Density Dr | Gmax (MPa) |
|---|---|---|---|
| Embankment fill | 20 | 0.85 | Eq. (1) |
| Dense sand | 20 | 0.73 | Eq. (1) |
| Loose sand | 19 | 0.42 | Eq. (1) |
| Sand and gravel | 20 | 0.66 | Eq. (1) |

The FLAC3D model comprises more than 65,000 hexahedral (brick) elements, established through the extrusion of a 2D plane strain model by a distance of 17 m in the out-of-plane direction. Element sizes range from 1 m to 2 m. The model's lateral boundaries were assigned as free field boundaries, while a compliant base condition was implemented at the model base.

The Landers (1992) earthquake was chosen for the modeling. This seismic record was applied at the base of the model in the form of a velocity time-history. The time-history, in turn, was converted into a shear stress time-history to serve as the actual earthquake input. The earthquake's acceleration time-history and spectrum acceleration are depicted in Figure 4.

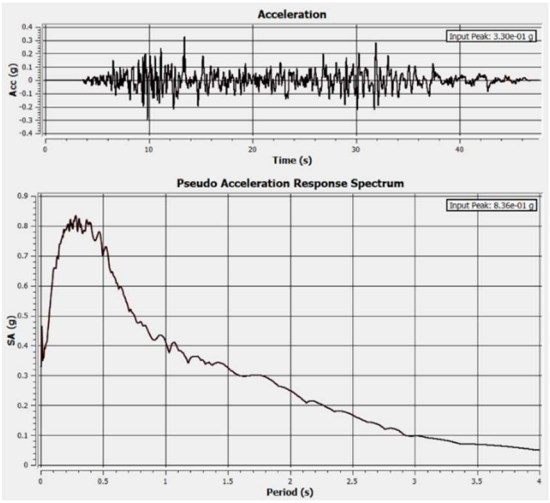


**Fig. 4**. Time-history and acceleration response spectrum of Landers (1992) earthquake

## Modeling Results

The post-seismic ground deformation is shown in Figure 5. The most substantial deformations, reaching approximately 2.4 m, were identified at the lower bench and river slope. Furthermore, lateral deformations of approximately 1 m manifested at the crest of the embankment.

The extent of soil liquefaction, expressed as the excess pore water pressure ratio Ru, is shown in Figure 6. Zones with Ru values larger than 0.9 are indicative of liquefaction. Liquefaction were primarily observed within the loose sand and sand and gravel layers.

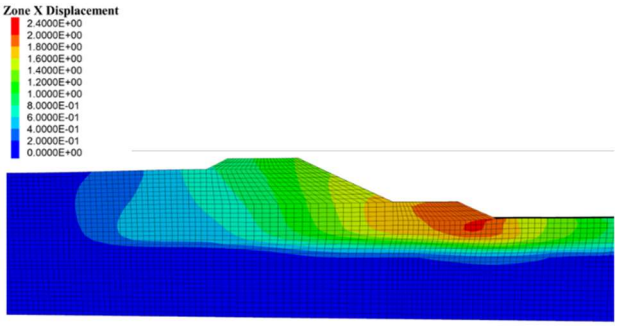


**Fig. 5**. Post seismic embankment deformation

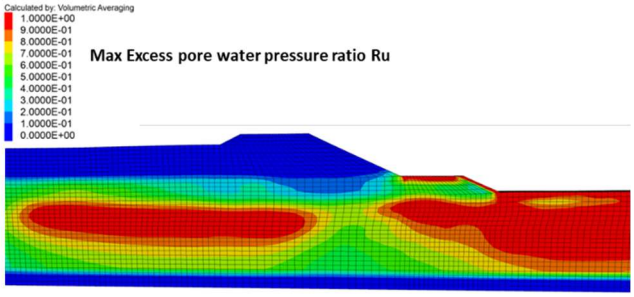


**Fig. 6**. Max excess pore pressure ratio (Ru)

## Comparison of Soil Models

The uniform geometry of the embankment model in the out-of-plane direction lends itself to a comparison of model responses between 2D plane strain and 3D scenarios. Figure 7 depicts the 2D and 3D responses of the P2PSand model, utilizing their respective 2D and 3D versions, by showcasing the time-history of horizontal deformation at the embankment crest. Impressively, the 2D and 3D P2PSand models exhibit strikingly similar outcomes.

Additionally, Figure 7 presents the response of the 2D geometry when using the PM4SAND model. Both the PM4SAND and P2PSand models share the same input parameters and undergo element test

calibration. However, it is noteworthy that the embankment deformation derived from the PM4SAND model slightly exceeds that from the P2PSand model.

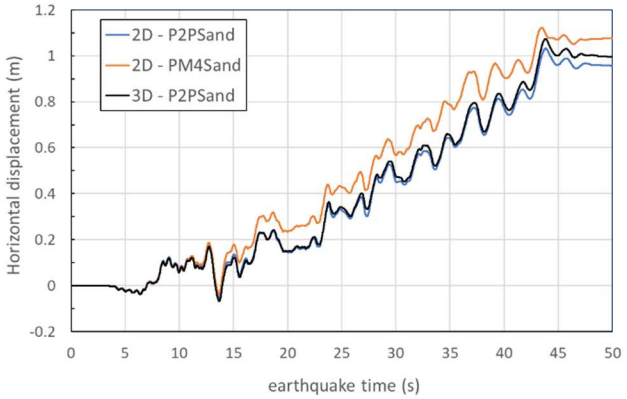


**Fig. 7**. 2D vs. 3D and PM4Sand vs. P2PSand comparisons – horizontal displacements at crest.

## Case Study 2: Anchored Quay Wall

### Geometry

To assess the seismic performance of an anchored combi-wall system, seismic soil-structure interaction analysis was conducted. The combi-wall serves to retain a soil height spanning from an elevation of 5.5 m (top of the wall) to -9 m (dredge level), totaling 14.5 m. Subsurface soil composition encompasses sand fill situated above an elevation of +1 m, underlain by a layer of loose sand, as well as a medium-dense mixture of gravel and sand. Subsequently, these are succeeded by a non-liquefiable stiff silt layer. Notably, during simulated earthquake events, the loose sand layer, and potentially portions of the gravel and sand layers, are prone to liquefaction.

For analysis of the earthquake-induced phenomena, the P2PSAND model was applied to simulate the behavior of liquefiable soils. The soil parameters and the corresponding constitutive models are consolidated in Table 2. Within the model, the water table was positioned at an elevation of +1 m. The geometric configuration of the model is shown in Figure 8.

**Table 2**. Soil parameters – case study 2

| Soil layer | Unit weight ($kN/m^3$) | Relative Density Dr | Gmax (MPa) |
|---|---|---|---|
| Compacted fill | 19 | 0.73 | Eq. (1) |
| Loose sand | 18.5 | 0.35 | Eq. (1) |
| Gravel and sand | 20 | 0.73 | Eq. (1) |
| Stiff silt | 18 | - | 150 |

The quay wall configuration comprises king piles with an outer diameter of 1422 mm and a thickness of 25 mm, constructed from steel pipe piles. These piles extend to the uppermost part of the gravel and sand layer, situated at an elevation of -25 m. Notably, the king piles are spaced with a center-to-center distance of 2.89 m.

Incorporated between the king piles are infill sheets of AZ26-700 type. These sheets extend from the top of the king piles to an elevation of -15 m.

Furthermore, the quay wall is reinforced through an anchor wall system that employs high-strength tie rods of ASDO 500 M125/115 specification. These tie rods establish connections between the king piles and the anchor wall. The anchor wall itself consists of sheet piles of AZ48-700 variety, positioned 30 m behind the quay wall. These sheet piles extend vertically from an elevation of +4 m to -4 m. The interplay of these components constitutes the overall configuration of the structures, as depicted in Figure 9a.

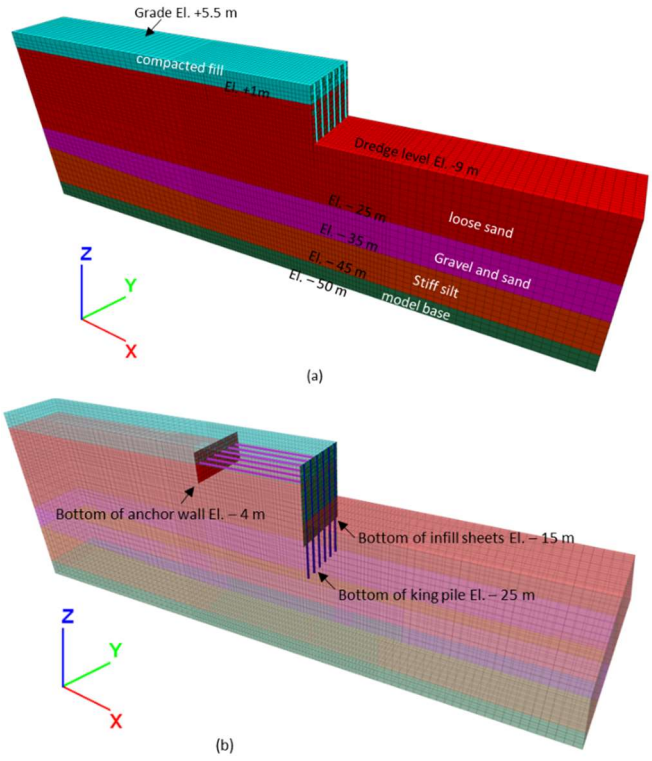


**Fig. 8**. (a) Quay wall geometry with filled zones filled, (b) Model geometry with transparent zones showing structures

## Earthquake Record

The purpose of this study is to demonstrate the capability of 3D modeling of soil-structure interaction modeling under seismic conditions and therefore, only one earthquake Tabas (Iran, 1978) was used as input time-history. The Tabas record and its response spectrum are shown in Figure 9b.

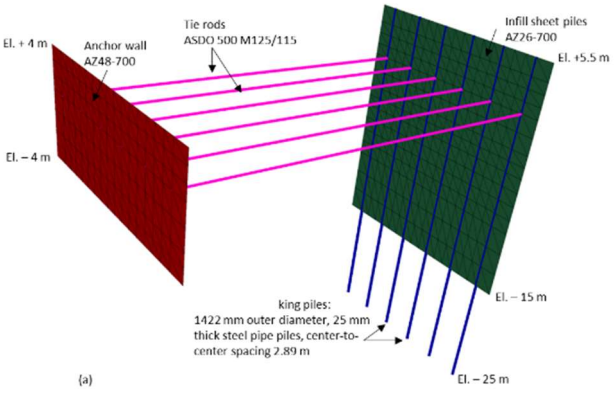


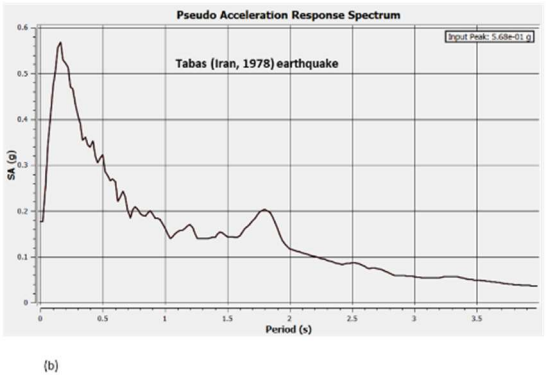


**Fig. 9**. (a) Quay wall structures, (b) Response spectrum of input earthquake record Tabas (Iran, 1978).

## Soil-Structure Interaction

The analysis encompassed coupled soil-structure interaction studies employing FLAC 3D. Hexahedral zones with a mixed discretization scheme were employed to model the soils. The quay wall's king piles were represented using pile elements, while liner elements captured the behavior of the infill sheets and anchor wall. Cable elements were used to simulate the tie rods. An interface friction angle of 17 degrees represented the interaction between soil and structure. The structures themselves were subjected to a full 3D model utilizing their actual properties.

The analysis unfolded in two distinct stages:

Stage 1: A static analysis was conducted to capture pre-earthquake conditions.

Stage 2: A dynamic analysis followed, where the model was subjected to earthquake motion. Shear stress time-histories were applied at the base of the model to replicate the earthquake's effect.

To minimize boundary-related effects, the FLAC model's lateral boundaries were extended on both sides. Lateral boundaries were defined with free-field conditions, while the model base was treated with a compliant base condition. Moreover, the simulation considered the hydrodynamic pressure exerted on the quay wall during earthquake. A surcharge of 12 kPa was applied on the ground surface behind the quay wall.

## Analysis Results - Existing Conditions

Under the existing soil conditions, the soil horizontal deformations at the end of the earthquake and maximum excess pore pressure ratio $R_u$ contours are shown in Figure 10. The results indicate largest soil displacements in the order of 1 m and soil liquefaction (Ru > 0.9) occurred behind the quay wall. The deformations of the quay wall and anchor wall are shown in Figure 11, which indicates a deflection of about 1 m at the top of the quay wall.

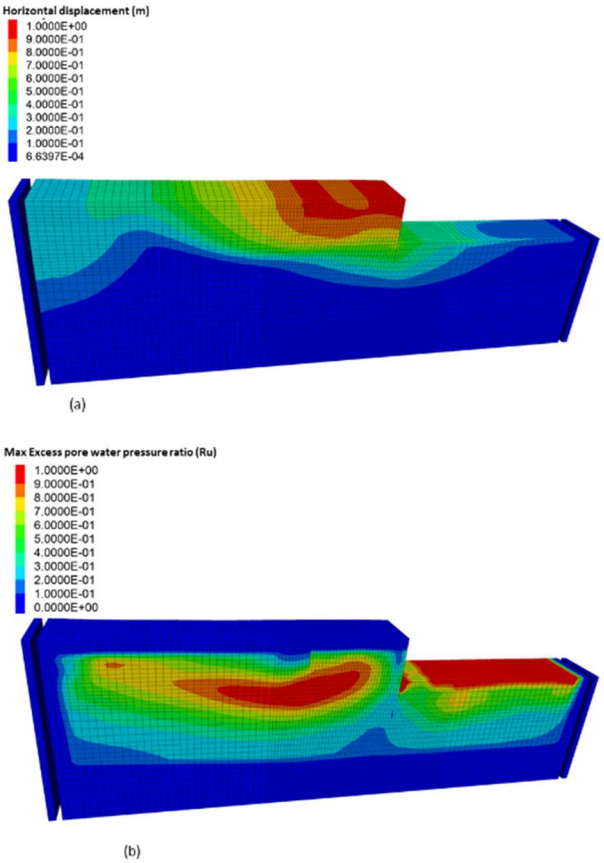


**Fig. 10**. Existing soil conditions (a) Soil horizontal displacement contours (m), (b) Max excess pore pressure ratio (Ru)

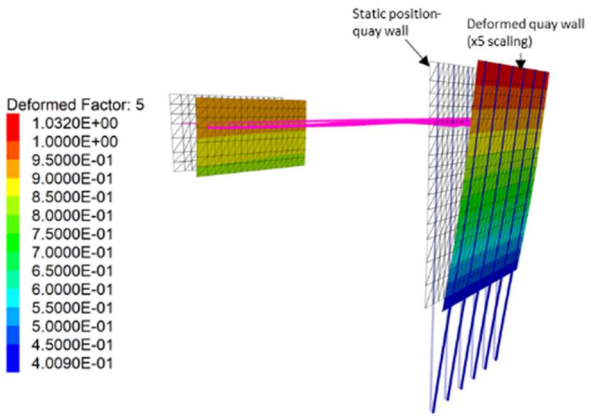


**Fig. 11**. Existing soil conditions - quay wall deformation (m),

## Effects of Earthquake Directions

The impact of earthquake directions was assessed through two distinct cases: one involving the earthquake applied in the X direction (perpendicular to the quay wall, i.e., from behind to in front of the quay wall), and the other involving the earthquake applied in the Y direction (out of the plane direction). Figure 12 provides a visualization of the horizontal displacements observed at the quay wall's top when the earthquake was induced in the X direction. Notably, the quay wall exhibited a deformation of approximately 1.05 m in the X direction, while displaying negligible deformation in the Y direction.

When the earthquake's force acted in the Y direction, the deformation of the quay wall in the Y direction mirrored the ground deformation at the model base. Consequently, the end-of-shaking Y-deformation remained relatively minor. Conversely, horizontal displacements of approximately 0.85 m manifested in the X direction. This degree of displacement is about 80% of the quay wall's deformation when subjected to an earthquake in the X direction.

The substantial quay wall deformation persisted even when the earthquake was directed out of the plane, rather than perpendicular to the quay wall. This can be attributed to the generation of excess pore water pressure within the soils, as showcased in Figure 13 for two points within the loose sand at about 20 and 55 m behind the quay wall. Notably, even when the earthquake was applied out of the plane, a smaller yet still significant pore water pressure was observed.

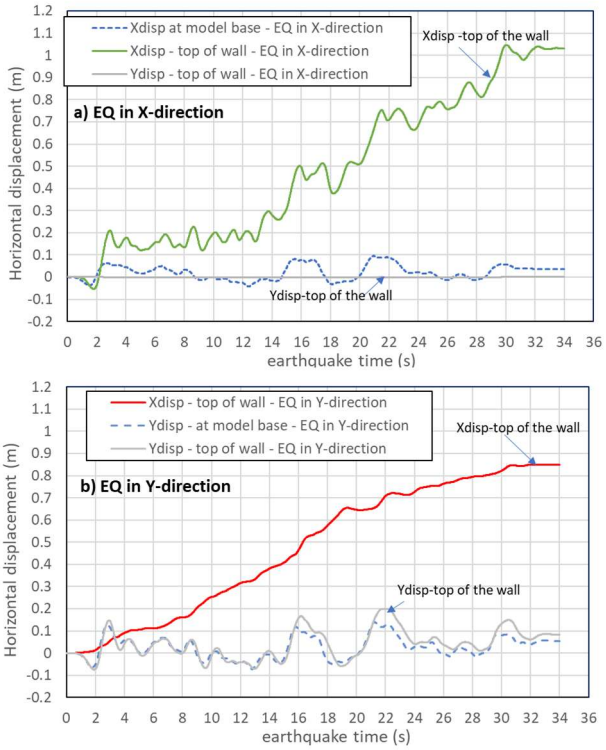


**Fig. 12**. Quay wall deformation time-histories a) Earthquake in the X-direction - onshore to offshore b) Earthquake in the Y-direction – out of plane

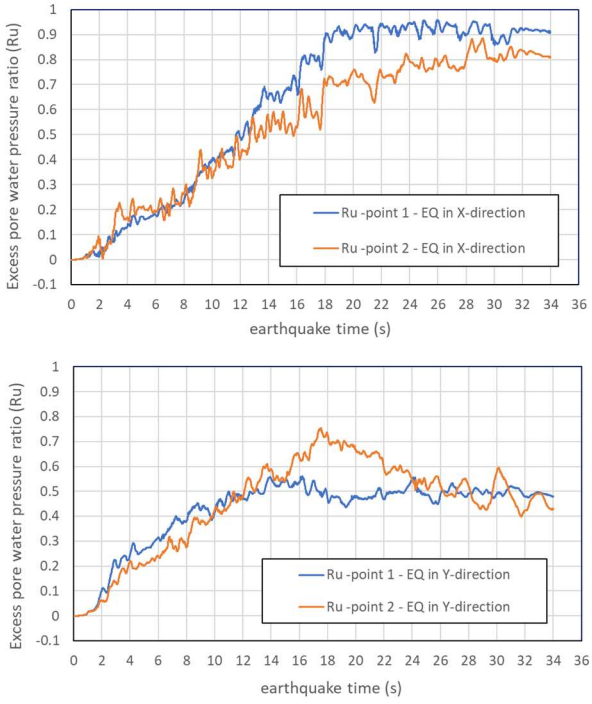


**Fig. 13**. Excess pore water pressure ratio time-histories a) Earthquake in X-direction and b) Earthquake in Y-direction

## Deep Soil Mixing Grids

Initial analyses have revealed substantial soil and structural deformation resulting from seismic activity, raising concerns about whether these deformations meet the practical project's performance-based design criteria. 3D modeling offers a notable advantage in representing real-world 3D deep soil mixing (DSM) grids. This approach contrasts with the conventional simplified 2D zones/columns, which lack the ability to capture the three-dimensional boxing effect.

Within the framework of this study, DSM grids measuring 10 m x 10 m and 7 m x 7 m square boxes were implemented both behind and in front of the quay wall. These grids were positioned beneath the compacted fill layer, situated below an elevation of +1 m in onshore areas, and below the dredge level (at an elevation of -9 m) in offshore areas. Notably, the DSM grids extended from the base of the compacted fill layer to the bottom of the loose sand layer, at an elevation of -25 m. Figure 14 presents a visual representation of the grids.

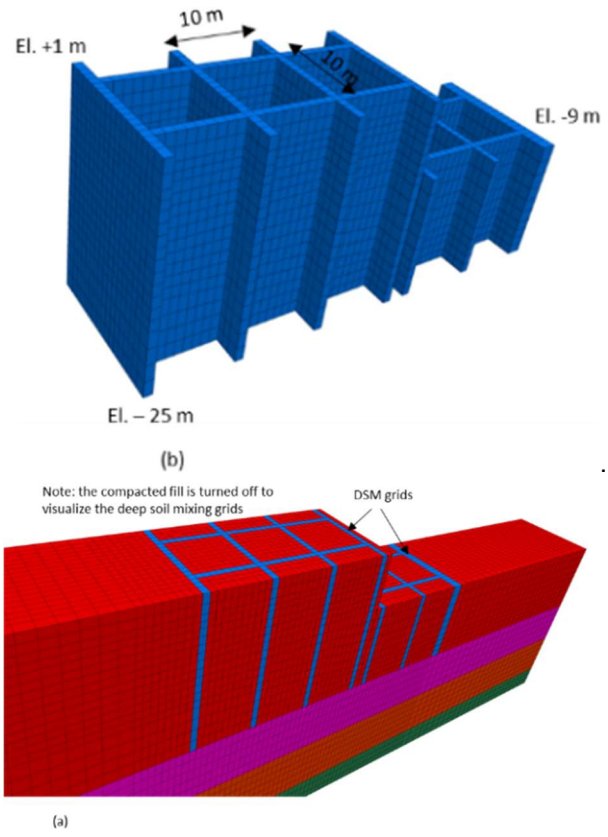


**Fig. 14**. (a) Soil reinforcement using deep soil mixing (DSM) grids, (b) DSM grids 10 m x 10 m

The modeling of these grids was undertaken using a Mohr-Coulomb model, characterized by a shear strength of 750 kPa. This value is derived from a representative unconfined shear strength $q_u$ of 1500 kPa specific to soil-cement mixing. Additionally, the secant modulus $E_{50}$ was set at $300q_u$, and the Poisson's ratio at 0.3.

Upon incorporating soil reinforcement through DSM grids of dimensions 10 m x 10 m, Figure 15 presents the outcomes in terms of soil displacements and Ru contours. Significantly reduced soil displacements, approximately 0.35 m, were projected behind the quay wall. It's noteworthy that no liquefaction was observed within the DSM boxes.

The DSM grids notably introduced a boxing effect, effectively constraining the development of excess pore pressure and soil displacement, particularly within the DSM boxes. This effect contributes to enhanced stabilization.

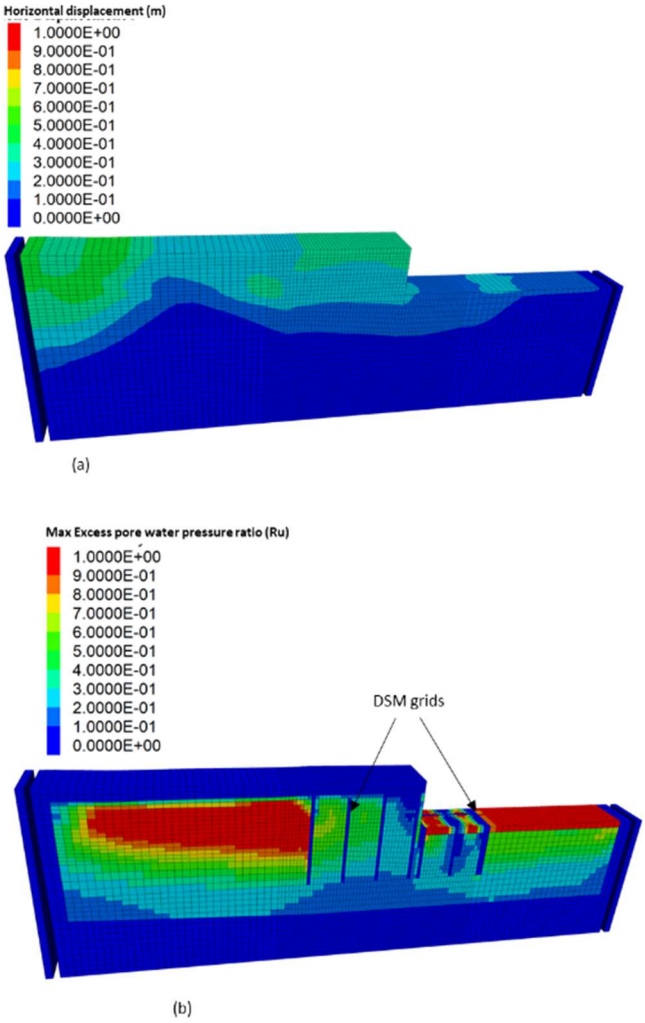


**Fig. 15**. DSM reinforcement 10 m x 10 m boxes (a) soil horizontal displacement contours (m), (b) max excess pore pressure ratio (Ru)

Comparing quay wall displacement time-histories with and without soil reinforcement, Figure 16 showcases the differential outcomes. With DSM grids measuring 10 m x 10 m, the wall displacement amounts to around 0.35 m. On the other hand, employing DSM grids measuring 7 m x 7 m yields a diminished displacement of 0.22 m. These deformations significantly undercut the 1 m estimate attained under existing soil conditions, i.e., without the integration of soil reinforcement.

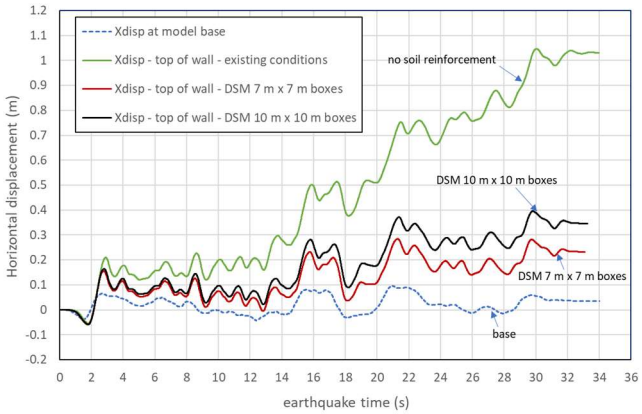


**Fig. 16**. Time-histories of quay wall displacements (top of wall) under existing soil conditions vs. DSM reinforcement conditions

## Spectral Acceleration at Ground Surface

Figure 17 illustrates the response spectra at the ground surface for both the existing conditions and those reinforced with DSM. The measurement point was positioned approximately 10 m behind the quay wall and within an existing soil column, rather than directly above the DSM grids. To provide comparison, the response spectrum of the input motion at the model's base is also incorporated in the figure.

Under the existing conditions, amplification was notably evident across various periods. This amplification extended to the peak ground acceleration (PGA), which was elevated from the input earthquake record's 0.18g to approximately 0.38g.

In contrast, the application of DSM reinforcement yielded a different scenario. For periods shorter than 0.5s, de-amplification occurred, resulting in a PGA of 0.15, slightly below that of the input earthquake record. This observed pattern suggests a reduction in shear stresses within the soil due to the heightened stiffness of the DSM shear boxes.

However, for periods exceeding 0.5s, amplification was observed. Notably, response spectra between the existing soil conditions and those fortified with DSM reinforcement exhibited similarities for periods beyond 0.5s.

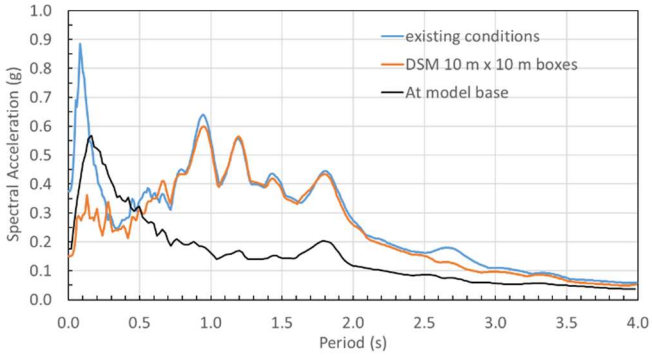


**Fig. 17**. Spectral accelerations at ground surface under existing soil conditions vs. DSM reinforcement conditions

# Case Study 3: Long Pier Structure

## Geometry

In this case study, we examined a long pier structure to assess its post-seismic deformation when subjected to substantial ground deformation along the nearshore slope due to liquefaction. The marine slope originates from the onshore area, characterized by a grade level at an elevation of +6 m. The slope extends towards the ocean, inclined at an approximately 4H:1V (horizontal to vertical) ratio. This slope has been dredged to an elevation of -11 m, positioned approximately 45 m away from the shoreline.

The subsurface soil composition encompasses compacted fill in the onshore region, followed by layers of loose to dense sand. These, in turn, are underlain by a stratum of stiff silt. Figure 18 presents the soil stratigraphy, while Table 3 provides the associated soil parameters.

The dimensions of the pier are approximately 198 m in length and 19 m in width. Notably, the deck's elevation rests at around El. 7 m. Comprising a total of 14 bents spaced 15 m apart, the pier features five bents situated on the nearshore slope. These nearshore bents are supported by a combination of vertical piles and inclined piles at a 1H:4V ratio. The remaining bents are upheld by vertical piles. All piles are steel pipe piles with an outer diameter of 1067 mm and a thickness of 19 mm. These piles extend down to an elevation of -45 m. Each bent is connected by a capping beam with dimensions measuring 1400 W x 1600 H. This beam serves to support the deck, offering an equivalent concrete thickness of 1.5 m. A visual representation of these structures is shown in Figure 18.

The Landers (1992) earthquake, same as that used in case study 1, was used as the input record for seismic soil-structure modeling.

**Table 3**. Soil parameters – case study 3

| Soil layer | Unit weight ($kN/m^3$) | Relative Density Dr | Gmax (MPa) |
|---|---|---|---|
| Compacted fill | 19 | 0.66 | Eq. (1) |
| Loose sand | 18.5 | 0.41 | Eq. (1) |
| Medium sand | 19 | 0.69 | Eq. (1) |
| Dense sand | 19 | 0.78 | Eq. (1) |
| Stiff silt | 18 | - | 150 |

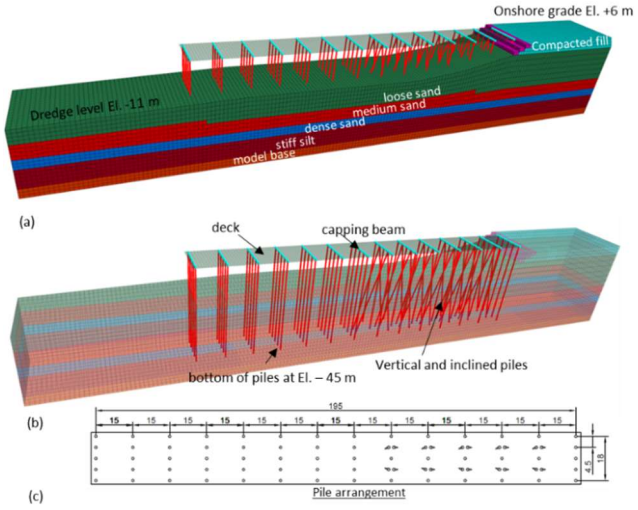


**Fig. 18**. (a) Pier geometry with filled zones filled, (b) Model geometry with transparent zones showing structures, (c) Pile arrangement

## Analysis Results

The outcomes of the analysis are demonstrated through two aspects: soil deformation at the earthquake's conclusion and maximum excess pore pressure ratio Ru contours, shown in Figure 19. Notably, Figure 19a employs a scaling factor of 5 to enhance visualization. Results indicate that the most substantial soil displacements occur along the nearshore slope, reaching magnitudes ranging from 1.5 m to 2 m. Liquefaction, denoted by Ru values exceeding 0.9, were prevalent within the sand layers (Figure 19b). Beyond the slope region, ground deformation diminishes, with values ranging between 0.2 m to 0.4 m in the flat dredged area.

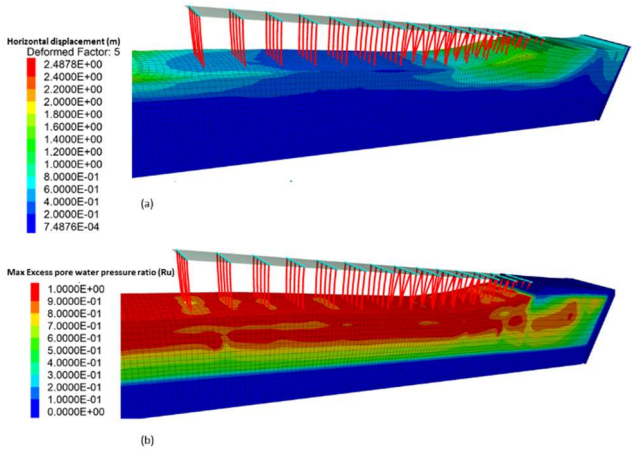


**Fig. 19**. (a) soil horizontal displacement contours (m), (b) max excess pore pressure ratio (Ru)

In Figure 20, the deformations of the structures are delineated. Closer proximity to the nearshore slope is linked to greater pile displacement, contrasting with the situation at the flat dredged area. Nevertheless, due to the interconnection of all piles with capping beams and the deck, which offer significant rigidity along the earthquake direction, pile displacements gravitated toward an intermediate range, approximating 0.5 m. This magnitude notably stands significantly lower than the most considerable soil displacements encountered along the nearshore slope.

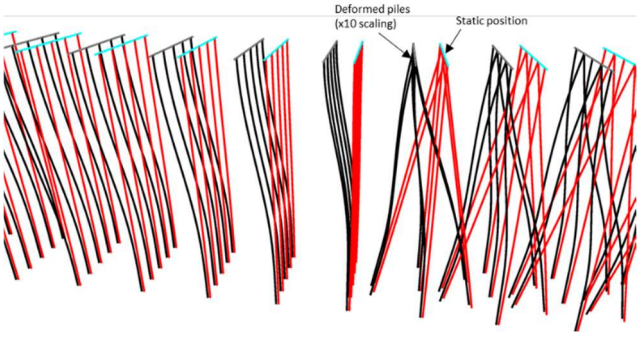


**Fig. 20**. Deformation of the piles

Displacement time-histories, both at the model's base and atop a representative pile, are presented in Figure 21. Importantly, the capping beams and the deck experienced practically identical displacements as the piles.

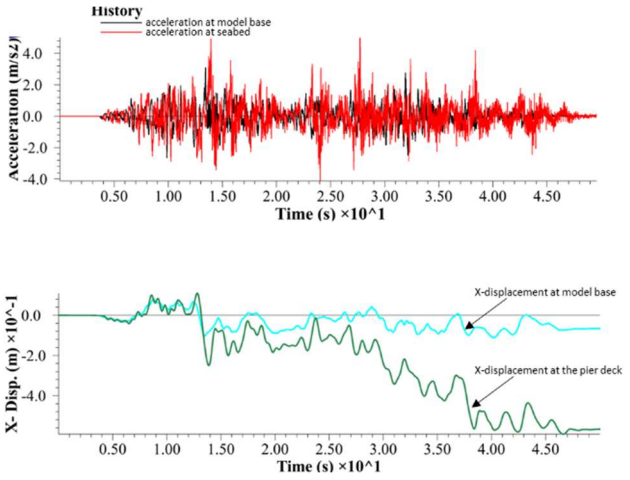


**Fig. 21**. (a) Acceleration time-histories, (b) X-displacement time-histories

## Conclusions

In this study, modeling of seismic response and soil-structure interaction for three distinct cases was conducted through advanced numerical modeling techniques. These cases encompassed an embankment dam on a liquefiable layer, an anchored quay wall system, and a long pier structure. The primary objective was to evaluate the potential impact of seismic events on these structures. The 3D modeling can simulate liquefaction patterns such as development of excess pore water pressure, liquefaction triggering, loss of strength, stiffness reduction and typical stress-strain loops using the 3D P2PSand model. The P2PSand model follows the state-of-the art theorical background and can be calibrated to widely used correlations and laboratory test results.

The application of deep soil mixing (DSM) grids, tailored to 3D geometry, demonstrated a remarkable capacity to restrain excess pore pressure and mitigate soil deformations. Notably, the de-amplification of spectral acceleration in certain periods under DSM reinforcement highlighted its efficacy in decreasing shear stresses within the soil, leading to improved seismic performance.

Furthermore, the investigation of a long pier structure emphasized the susceptibility of marine slopes to seismic events and the subsequent deformation of the structure. Here, the interplay between soil deformation and structural response showcased the interconnected nature of the two factors. The integration of inclined and vertical piles, along with capping beams, illustrated the capacity to mitigate pile displacement through a distributed structural system.

## References

Elgamal, A., Yang, Z., Parra, E., & Ragheb, A. (2003). Modeling of cyclic mobility in saturated cohesionless soils. International Journal of Plasticity, 19(6), 883-905.

Yang, Z., Elgamal, A., & Parra, E. (2003). Computational model for cyclic mobility and associated shear deformation. Journal of Geotechnical and Geoenvironmental Engineering, 129(12), 1119-1127.

Dafalias, Y. F., & Manzari, M. T. (2004). Simple plasticity sand model accounting for fabric change effects. Journal of Engineering mechanics, 130(6), 622-634.

Taiebat, M., & Dafalias, Y. F. (2008). SANISAND: Simple anisotropic sand plasticity model. International Journal for Numerical and Analytical Methods in Geomechanics, 32(8), 915-948.

Yang, M., Taiebat, M., & Dafalias, Y. F. (2022). SANISAND-MSf: a sand plasticity model with memory surface and semifluidised state. Géotechnique, 72(3), 227-246.

Papadimitriou, A. G., & Bouckovalas, G. D. (2002). Plasticity model for sand under small and large cyclic strains: a multiaxial formulation. Soil Dynamics and Earthquake Engineering, 22(3), 191-204.

Beaty, M. H., & Byrne, P. M. (2011). UBCSAND constitutive model version 904aR. Itasca UDM Web Site.

Boulanger, R. W., & Ziotopoulou, K. (2015). PM4Sand (Version 3): A sand plasticity model for earthquake engineering applications. Center for Geotechnical Modeling Report No. UCD/CGM-15/01, Department of Civil and Environmental Engineering, University of California, Davis, Calif.

Cheng, Z., & Detournay, C. (2021). Formulation, validation and application of a practice-oriented two-surface plasticity sand model. Computers and Geotechnics, 132, 103984.

Idriss, I. M., & Boulanger, R. W. (2008). Monograph MNO-12: Soil liquefaction during earthquakes. Earthquake Engineering Research Institute, Oakland, CA.